




PACMan: A software package for automated single-cell chlorophyll fluorometry

Olle Pontén^{1,2}  | Linhong Xiao¹ | Jeanne Kutter¹ | Yuan Cui¹ |
 Carolina Wählby³  | Lars Behrendt¹ 

¹Department of Organismal Biology, Science for Life Laboratory, Uppsala University, Uppsala, Sweden

²School of Mathematics & Statistics, The University of Melbourne, Parkville, VIC, Australia

³Department of Information Technology and Science for Life Laboratory, Uppsala University, Uppsala, Sweden

Correspondence

Lars Behrendt, Science for Life Laboratory, Department of Organismal Biology, Uppsala University, Norbyvägen 18A, 75236 Uppsala, Sweden.

Email: lars.behrendt@scilifelab.uu.se

Funding information

Carl Tryggers Stiftelse för Vetenskaplig Forskning; Science for Life Laboratory; Svenska Växtgeografiska Sällskapet; Vetenskapsrådet

Abstract

Microalgae, small photosynthetic unicells, are of great interest to ecology, ecotoxicology and biotechnology and there is a growing need to investigate the ability of cells to photosynthesize under variable conditions. Current strategies involve hand-operated pulse-amplitude-modulated (PAM) chlorophyll fluorimeters, which can provide detailed insights into the photophysiology of entire populations- or individual cells of microalgae but are typically limited in their throughput. To increase the throughput of a commercially available MICROSCOPY-PAM system, we present the PAM Automation Control Manager ('PACMan'), an open-source Python software package that automates image acquisition, microscopy stage control and the triggering of external hardware components. PACMan comes with a user-friendly graphical user interface and is released together with a stand-alone tool (PAMalysis) for the automated calculation of per-cell maximum quantum efficiencies ($= F_v/F_m$). Using these two software packages, we successfully tracked the photophysiology of >1000 individual cells of green algae (*Chlamydomonas reinhardtii*) and dinoflagellates (genus *Symbiodiniaceae*) within custom-made microfluidic devices. Compared to the manual operation of MICROSCOPY-PAM systems, this represents a 10-fold increase in throughput. During experiments, PACMan coordinated the movement of the microscope stage and triggered the MICROSCOPY-PAM system to repeatedly capture high-quality image data across multiple positions. Finally, we analyzed single-cell F_v/F_m with the manufacturer-supplied software and PAMalysis, demonstrating a median difference <0.5% between both methods. We foresee that PACMan, and its auxiliary software package will help increase the experimental throughput in a range of microalgae studies currently relying on hand-operated MICROSCOPY-PAM technologies.

KEYWORDS

Chlamydomonas reinhardtii, microalgae, microfluidics, microscopy automation, MICROSCOPY-PAM, pulse-amplitude-modulated chlorophyll fluorometry, *Symbiodiniaceae*

This is an open access article under the terms of the [Creative Commons Attribution-NonCommercial](https://creativecommons.org/licenses/by-nc/4.0/) License, which permits use, distribution and reproduction in any medium, provided the original work is properly cited and is not used for commercial purposes.

© 2023 The Authors. *Cytometry Part A* published by Wiley Periodicals LLC on behalf of International Society for Advancement of Cytometry.

1 | INTRODUCTION

Chlorophyll fluorometry is a widely used fluorescence-based technique to study plant and algae photophysiology at the macro- and micro-level [1–3]. This non-invasive technique has provided data on important photophysiological processes within a range of phototrophs and has been a crucial tool for researching plant physiology and the effects of climate change [4–6]. PAM is also frequently used within agricultural sciences to select crops with desirable photophysiological characteristics such as decreased sensitivity to herbicides [6]. The majority of PAM systems apply pulse-amplitude-modulated flashlets of non-actinic light to measure the minimal fluorescence of photosystem II (PSII) reaction centers ($= F_0$) and apply a strong saturation pulse (SP) to saturate PSII and measure its maximal fluorescence emission ($= F_m$). Notably, pulse-amplitude modulation enables measurements of these two parameters under both darkness and actinic light. This enables the application of PAM to calculate, among many parameters, (i) the maximum quantum efficiency of PSII under dark ($F_m - F_0 / F_m$, also expressed as F_v / F_m) and (ii) the effective quantum yield of PSII, $F_m' - F_0' / F_m'$, during application of actinic light. Decreases in F_v / F_m are regarded as a good proxy for photophysiological stress [1] as it describes the capacity of cells to perform photosynthesis. F_v / F_m is defined according to Equation (1), where $F_v = F_m - F_0$ [1, 7] unless if $F_m - F_0 < 0$ in which case $F_v = 0$.

$$F_v / F_m = \frac{F_m - F_0}{F_m} \quad (1)$$

For a more in-depth description of the mechanics, principle of operation and other possible parameters to calculate from PAM chlorophyll fluorometry data we direct readers elsewhere [1].

Among the most common chlorophyll fluorometry systems is the IMAGING-PAM series from Walz. These systems allow operators to repeatedly probe photophysiological parameters of photosynthetic organisms, including agricultural crops [6], wild plants [8] and microalgae [9, 10]. The MICROSCOPY-PAM version is often used for researching phototrophs at the microscale, yet both the hardware and software of this system remains hand-operated, which severely limits the throughput of this platform. Since the advent of microscopy, one of the goals has been to increase both the quality and the quantity of data accessible to imaging modalities. For modern instruments, this often takes the form of motorization and the addition of computer-controllable components, which provide researchers with increasing control across multiple dimensions (e.g., time, space and imaging mode). Today most commercial, research-grade microscopes come with costly and proprietary software that enable users to operate such advanced features. These software packages increase the quantity and quality of data that can be obtained while reducing the number of experiments which reduces reagents, variability and labor costs. In addition to commercial software there are open-source software alternatives, for example, the widely used μ -Manager [11], that employs extensive libraries of device-adapters to allow generic control over many imaging instruments and varying auxiliary hardware.

In order to increase the experimental throughput of the commonly used MICROSCOPY-PAM system, we present a software suite that automates complex experiments (PACMan) and analyses the resulting imaging data (PAMalysis). Here, we tested the ability of this software suite to track PSII efficiencies in hundreds of single cells over time and under different exposures to environmental stress within previously designed microfluidic devices [9].

2 | MATERIALS AND METHODS

2.1 | Cell culture conditions and strains

All cultures were grown in an Algaetron AG 230 incubator (Photon System Instruments, Czech Republic) under LED lights providing broad spectrum (400–700 nm) irradiance at $100 \mu\text{mol photons m}^{-2} \text{s}^{-1}$ in a day/night cycle of 14 h/10 h at 22°C . *Symbiodiniaceae* cultures were obtained from the Bigelow culture collection and cultures of *Chlamydomonas reinhardtii* were supplied by Professor Paul Hudson (Division of Systems Biology, KTH, Sweden). All cultures were non-axenic and no antimicrobial agents were added at any point. *Symbiodiniaceae* cultures were grown in f/2 medium prepared from autoclaved and filtered (bottle-top vacuum filter, $0.2 \mu\text{m}$, Corning, USA) artificial seawater (36 ppt, Instant Ocean, Aquarium Systems, Sarrebourg, France). Following sterilization, the following components were added to 1 L of artificial seawater: NaNO_3 (75 g L^{-1} , 1 mL), $\text{NaH}_2\text{PO}_4 \cdot \text{H}_2\text{O}$ (5 g L^{-1} , 1 mL), $\text{Na}_2\text{SiO}_3 \cdot 9\text{H}_2\text{O}$ (30 g L^{-1} , 1 mL), trace metal solution (1 mL), and vitamin solution (0.5 mL). *C. reinhardtii* was grown in Tris-Acetate-Phosphate medium (Thermo Fischer Scientific Inc.). All experiments were performed using cultures in the mid-exponential growth phase as previously determined by measuring the optical density of cultures in a Spark multimode microplate reader at 680 nm (Tecan Trading AG, Switzerland).

2.2 | Manufacturing and loading of microfluidic devices

The design and manufacturing of microfluidic devices used throughout the study are published in [9], but are described in brief (Figure S1). Briefly, silica wafers with embossed patterns were manufactured using standard photolithographic techniques. Silica wafers were covered with Sylgard 184 (Sigma-Aldrich, USA) polydimethylsiloxane (PDMS) prepolymer mixed at a 1:10 ratio of curing agent to monomer. After curing in an oven for 12 h at 80°C the PDMS devices were excised manually by scalpel. The PDMS surfaces were covered in Scotch tape and the devices were then bonded to microscopy slides, previously cleaned with 70% ethanol, via O_2 plasma treatment (Zepto 1, Diener Electronics GmbH). The plasma treatment lasted for 20 s at 50% power and to increase bond stability the device was left to rest on an 80°C hotplate for >2 h.

Cell loading is described in detail in [9] but is briefly presented. Microfluidic devices were placed in vacuum for 5–20 min and then

injected with sterile f/2 medium. For loading, 2–4 mL of mid-exponentially growing cells were centrifuged at 1500 rcf and the supernatant was discarded. The remaining cell pellet was carefully re-suspended in 250–500 μL of sterile medium and concentrated cells were then injected into the microfluidic devices using a pipette. Following the introduction of cells, the microfluidic device was manually compressed with a pair of forceps, creating compression and suction forces that deposited cells into microwells (diameter: 20 μm , depth: 15 μm). Within the main channel of the microfluidic device, these microwells ($n = 6000$ –16,000, depending on the design) are organized in rectangular arrays. Well dimensions were previously determined to accommodate microalgae cells at most life stages without damaging them, and to yield a good ratio between wells containing a single cell, multiple cells, or being empty [9].

2.3 | Generation of chemical gradients within microfluidic devices

Within microfluidic devices, chemical concentration gradients were generated via the gradual and controlled mixing of two fluid streams via a Christmas tree concentration gradient generator (CGG, see Figure S1 for device design). The gradient was first characterized by injecting f/2 medium laced with and without fluorescein (1 μM , SIGMA) in the two inlets. After mixing, the liquids exit the gradient generator through 10 outlets which are immediately connected to the evenly spaced array of microwells. This microwell arena is 375 μm wide, 7000 μm long and encompasses 1600 wells with a defined chemical concentration in the entire area, excluding a narrow border region. To ensure that the gradient was stable the gradient was let to run for 30 min and was subsequently imaged using a fluorescence microscope (Ex. 465–495 nm, Em. 495–555 nm, Nikon Ti2-E, Nikon, Japan). The resulting, location-dependent fluorescence intensity was used to calculate the concentration of fluorescein in each lane of wells (see Figure S1). Chemical gradients were established between f/2 medium with ($= 10 \mu\text{g L}^{-1}$) and without ($= 0 \mu\text{g L}^{-1}$) the herbicide *N'*-(3,4-dichlorophenyl)-*N,N*-dimethylurea (DCMU, Sigma-Aldrich), each introduced separately into one of the inlet ports of the chemical gradient generator (Figure S1).

To maximize accuracy, the same syringes, tubing and microfluidic device were used both for device characterization (via fluorescein) and subsequent exposure of cells to DCMU.

2.4 | Supply of media and chemicals during microfluidic experiments

Media was supplied into microfluidic devices via 25 mL Cetoni glass syringes (Cetoni, GmbH) mounted onto a Cetoni Low Pressure syringe pump controlled by Q-Mix Elements (version 20,190,821, Cetoni, GmbH). Flow rates were kept at a constant rate of 800 $\mu\text{L}/\text{hour}$ and connected to microfluidic inlet ports with a 0.508 mm ID/1.524 mm OD Tygon microfluidic tubing (Saint-Gobain Performance Plastics). In

earlier experiments, this flow rate was determined to elicit no adverse biological reactions among *Symbiodinaceae* cells [9].

2.5 | MICROSCOPY-PAM setup

A microscopy-based chlorophyll fluorimeter imaging system (IMAG-RGB, Heinz Walz GmbH, Effeltrich, Germany) was used to quantify the photosynthetic activity of individual microalgae. This system is hereafter referred to as “MICROSCOPY-PAM”. This microscope system provides RBG light to cells via a liquid light guide mounted onto a manually operated microscope (Zeiss Axioscope A1, Carl Zeiss AG), is equipped with an IMAG-K6 camera (Allied Vision Technologies) and connected to the PAM CONTROL unit via a Firewire cable. In its standard configuration this system has been described in great detail [12].

Unless otherwise specified, a 10 \times Zeiss Fluor 10 \times /0.5 objective was used to capture all images in this study. To achieve automatization, the standard microscopy configuration (above) was augmented with a motorized microscope stage (H101A, Prior Scientific Ltd), a PS3H122 Focus Driver (Prior Scientific Ltd), and a Heidenhain Model MT1281 linear focus encoder with a resolution of 0.2 μm . The PS3H122 was further augmented with a custom-made 3D-printed connector piece (Figure S2) to reduce Z directional backlash and slippage. All components were controlled by a PRIOR ProScan III Controller (Prior Scientific Ltd). This setup enables repeatable and precise XY ($\pm 1 \mu\text{m}$) and Z (0.002 μm) movements.

In its standard configuration, MICROSCOPY-PAM is operated via the ImagingWin software. ImagingWin runs on a computer with Windows 7/8/10, connected to the PAM CONTROL unit via a USB-A cable. ImagingWin provides manual control over SPs, records data, performs image analysis and provides scripting capabilities via its own scripting language. This software also contains a timer where the software will automatically apply SPs and record data at desired intervals. ImagingWin has its own image format, the closed .pim format, but can also export but not read data to/from Tagged Image Format files (.tif) or .jpg files. In .pim images, fluorescence values are stored as values between 0.001 and 1.0 and when exported as .tif images they are stored as grayscale 8-bit images with intensity values between 0 and 255. Importantly, .pim images cannot be concatenated, implying that additional experimental data cannot be appended after a measurement series has finished. The version 2.51 [13] implemented remote operation via a COM server connection, and this version of the software has been used throughout the experiments presented here.

2.6 | PACMan automates microscope components and is operated via GUI

Due to the availability of diverse packages for scientists and simplicity of its syntax, PACMan was written in Python. PACMan can be installed on systems using Windows 7, 8, or 10 via the Python Index Wheel format. The main prerequisite software needed is ImagingWin (version 2.51) and Python 3.8.

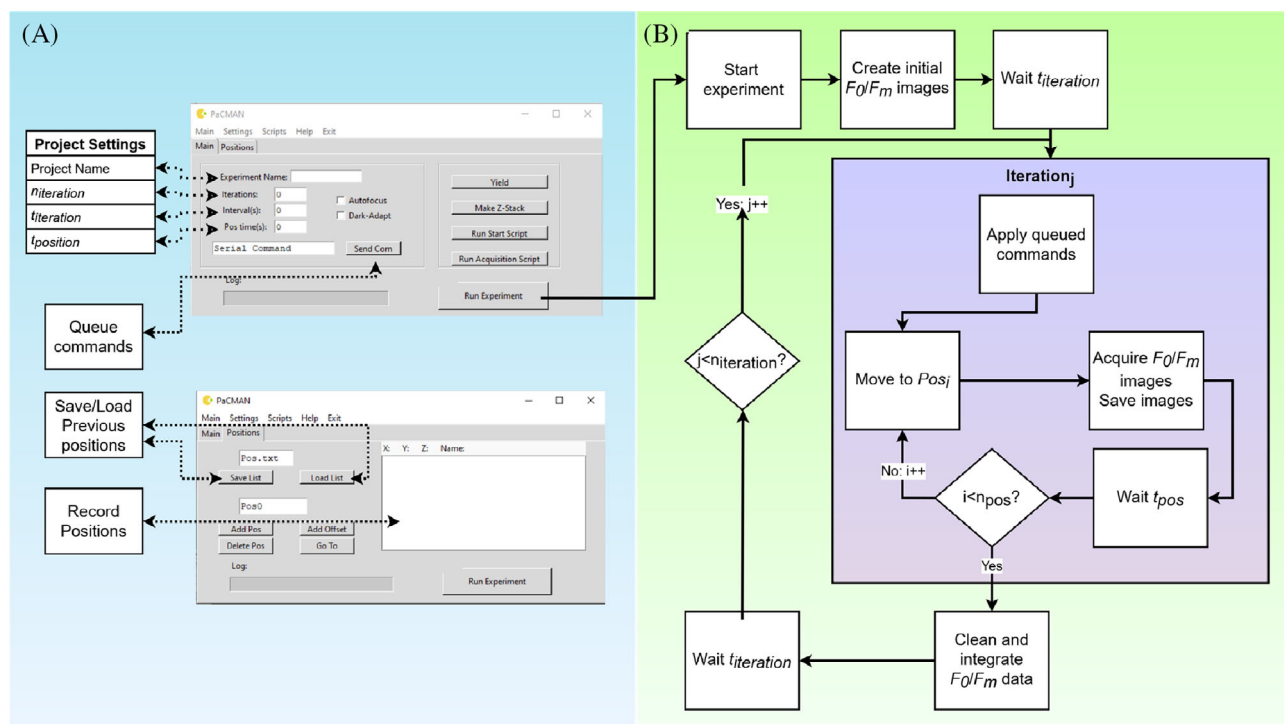


FIGURE 1 Overview of PACMan (A) The two different subpanels of the PACMan GUI. In the main panel (Top) the operator chooses the experiment name, number of iterations ($n_{\text{iteration}}$), wait time between iterations ($t_{\text{iteration}}$) and the wait time between each position (t_{position}). Commands can be queued to be applied at certain iterations, allowing for changing of light intensities or waiting periods automatically during the experiment. (Bottom) In the positions panel, XYZ positions can be added, offset and deleted manually. The operator can also load previously saved positions with the “Load List” button or save the current list to a text file using the “Save List” button. (B) Schematic view of the PACMan algorithm and how it performs experiments. An operator first enters project settings and selects positions and then presses the “Run Experiment” button. PACMan then moves the stage between positions, acquiring images at each position. Between each position, PACMan waits t_{position} seconds. After all positions have been traversed PACMan will wait $t_{\text{iteration}}$ and during this period it will reorder the data acquired during the previous round. When a new round starts, PACMan will check if there are any queued commands and if so execute them before moving to the first position. This continues until PACMan has performed $n_{\text{iteration}}$ acquisition rounds. [Color figure can be viewed at [wileyonlinelibrary.com](https://onlinelibrary.wiley.com/doi/10.1002/cyto.a.24808)]

The general runtime algorithm for PACMan is conceptually simple (Figure 1B). PACMan moves sequentially between microscope stage positions (saved in a list), applies a SP at each position and saves the resulting image data. Between every position, PACMan waits a user-defined amount of time ($= t_{\text{position}}$). After all positions have been visited PACMan again waits a user-defined amount of time ($= t_{\text{iteration}}$) during which it concatenates the newly saved image data onto the previous images from the same position and annotates these with system metadata such as stage XY position. After this it moves back to the first position and repeats imaging until every position has been visited a specified number of iterations ($= n_{\text{iteration}}$).

The PACMan software is made up of a graphical user interface (GUI) and three principal components: the main coordinating PACMan Module, the Stage Communicator Module (SCM) and the IPAM Remote Handler Module (IRHM).

The GUI (Figure 1A) contains two panels, with the first one used for entering project parameters, such as the name of the experiment, $n_{\text{iteration}}$, $t_{\text{iteration}}$ and t_{position} . The second panel is used for recording positions. When the operator has identified a desirable position, the operator can add its coordinates to a list of positions via the “Add Pos” button. These coordinates represent the XYZ positions that

PACMan will move to when performing image acquisition. After all settings (Figure 1A) and positions have been recorded, the experiment is started with the “Run Experiment” button.

The main module (PACMan) records operator-entered data via the GUI, reorganizes image data and is responsible for coordinating the other modules of the software. The recorded image data is saved as 8-bit .tif image stack files with one .tif file per selected position. Additionally, a detailed experimental log is saved as a text file.

When an experiment has started, the main PACMan module coordinates the movement of the stage via the SCM. with the application of saturation pulses, and the recording of image data via the IRHM. The hierarchy between these modules is shown in Figure 2 and their functionality explained below.

The SCM connects to a user-specified communication (COM) port which addresses the stage controller (Figure 2A). The SCM sends serial commands to the microscope stage controller, which then interprets and moves the microscope stage accordingly. The IRHM communicates to a running ImagingWin instance which controls the MICROSCOPY-PAM system (Figure 2A). The connection itself is handled, analogously to the SCM system, as a serial connection where the ImagingWin software acts as a server accepting commands from a

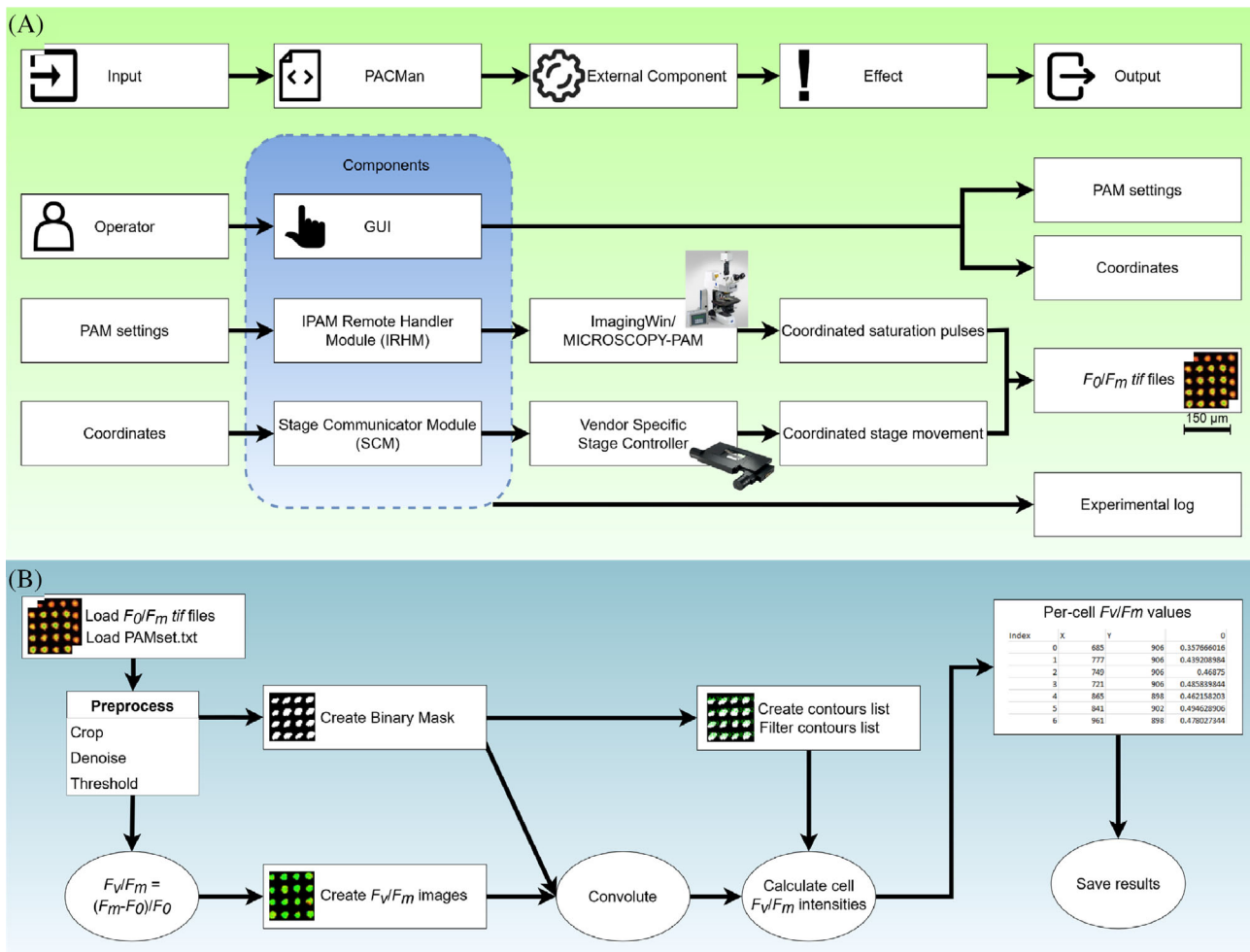


FIGURE 2 Schematic flowchart of PACMan and PAMalysis. (A) Flow diagram of how PACMan is organized internally and interacts with external parts of the system. The operator enters experimental parameters into a GUI (see Figure 1). PACMan uses these parameters to coordinate the Stage Communicator Module (SCM) which moves the stage and directs the IPAM Remote Handler Module (IRHM) to send commands to ImagingWin to trigger saturation pulses, take F_0/F_m images and export data as .tif files. PACMan also keeps a detailed experimental log. (B) Flowchart of image processing steps implemented in PAMalysis. First F_0/F_m images and PAMset.txt is loaded and F_v/F_m images are calculated according to Equation (1) (see main text). Following data loading, binary masks are created to remove noise and segment cells. Cells, represented as a list of contours, are calculated and indexed based on this mask as well as filtered based on size. Median F_v/F_m values are calculated for each cell and saved in the form of text files. Each cell is assigned an index (corresponding to its index in the cell mask) with its position and F_v/F_m at every frame saved. For multiple-position experiments both per-position files and a complete file containing data from all positions are saved. [Color figure can be viewed at [wileyonlinelibrary.com](https://onlinelibrary.wiley.com)]

client (= PACMan). Any command sent to the ImagingWin software is made up of two parts, (i) an obligatory command part and (ii) an optional parameter part. The commands used by the IRHM are listed in the MICROSCOPY-PAM manual [13]. The ImagingWin instance is not exclusively controlled by the remote handler and can be manually operated at the same time.

2.7 | PAMalysis performs automated cell segmentation and calculates F_v/F_m

Compared to manual data generation, PACMan significantly increases the amount of output data by covering multiple fields of views over

time in a single experiment. To analyze the resulting data we developed PAMalysis, a stand-alone tool for the calculation of per-cell maximum quantum efficiencies in darkness, F_v/F_m . PAMalysis takes F_0/F_m images, converts them into F_v/F_m images, segments regions of interests (ROIs) and calculates the average F_v/F_m intensity of these ROIs (detailed in Figure 2B). The final output of PAMalysis is a text file containing per-cell values of F_v/F_m and (optional) graphical presentations of the distribution of a populations F_v/F_m values at a single time point and a line graph of the mean F_v/F_m over the entire experiment (Examples shown in Figure 5). Unlike PACMan, PAMalysis does not have a GUI and is executed as a Python script. PAMalysis can be executed in batch mode, analyzing all F_0/F_m image stacks in a folder, or it can analyze a single stack identified by filename.

Within PAMalysis there are a number of user-defined settings (underlined in this section). These settings must be supplied by the user in a text file (by default called PAMset.txt) and provided to PAMalysis in order to customize the analysis to the specific experiment (a PAMset file with default values for most settings is supplied with the software). These settings are listed in full in Table S1.

The maximum quantum efficiency, F_v/F_m , (defined in Equation (1)) is currently the only parameter that PAMalysis calculates. This parameter can be calculated on a per pixel basis for any given F_0/F_m image data, making it suitable for automated analysis. By segmenting the F_v/F_m images appropriately we can then define per-cell F_v/F_m values at any given time. The F_v/F_m value of a cell at frame t is defined as the mean F_v/F_m pixel intensity over the area of the cell at frame t .

PAMalysis performs cell segmentation and calculates F_v/F_m for each cell (Figure 2B) via the following steps. First, F_0/F_m images are read as an 8-bit image stack of 480 by 640 pixels and $4 + n_{\text{iteration}} \times 2$ frames, with each stack corresponding to a single position. The first four frames are initial F_0 (i), F_m (ii), brightfield (iii), and a near-infrared image (iv), while each of the following frames contain alternating F_0 and F_m images. In the next step, these image stacks are used to create one denoising mask per F_0/F_m stack. This is done by applying an intensity threshold of 10 to all F_0 images and convoluting the result with a median filter ($k = 3$). These operations eliminate low-intensity and salt-and-pepper noise, respectively. In a third step, the resulting image stack is summed and converted into a binary mask (Figure 2B).

Finally, the F_v/F_m for every F_0/F_m image pair is calculated according to Equation (1) and the resulting image is multiplied with the previously created binary mask, resulting in a noise-dampened F_v/F_m image. This image is then combined with a list of cell contours which is generated according to the procedure below.

PAMalysis performs cell segmentation by one of two methods. The F_0 method (“Ft_Masks” in PAMset) uses F_0 images to determine the location and area of microalgae cells. The F_v/F_m projection (“Projection”) method instead uses a projection of the calculated F_v/F_m images, identifying them based on their summed fluorescence response intensity to a saturation pulse. These two methods use the same algorithm to perform the final cell segmentation but differ in how they create the mask for finding cell contours.

Segmentation via F_0 images progresses through the following steps:

1. To all $F_{0,j}$ images a thresholding operation with a value of User_threshold is applied, with $\{0 < j < t\}$.
2. An intensity projection of all thresholded F_0 images is created: $F_{0,All}$
3. Any pixel in $F_{0,All}$ with an intensity above 0 is set to 1, creating a binary mask.
4. To the binary mask a contour finding algorithm [14] is applied, which returns a list of all contours.
5. This list is filtered by size so that only a list of all contours (length n_{cells}) with an area between [Minsize, Maxsize] remain.

Segmentation via F_v/F_m intensity projection image progresses through the following steps:

1. An intensity projection of all F_v/F_m images is created: Y_{All}
2. A thresholding operation is applied to Y_{All} with a value of $n_{\text{iteration}} \times \text{User_threshold}$.
3. Any pixel in the thresholded Y_{All} image with an intensity above 0 is set to 1, creating a binary mask.
4. To the binary mask a contour finding algorithm [14] is applied, which returns a list of all contours.
5. This list is filtered by size so that only a list of all contours (length n_{cells}) with an area between [Minsize, Maxsize] remain.

The noise-filtered F_v/F_m images and the list of contours are used to calculate bounding rectangles for every cell and then finally to calculate the F_v/F_m of every cell.

1. From contour_j construct rectangle_j so that the entirety of contour_j fits in rectangle_j , then add border of 1 pixel to all sides. The four sides of the rectangle are called B, T, L, R
2. For every rectangle_j , calculate the mean intensity (I) of every non-zero pixel according to Equation (2).

$$\frac{F_v}{F_{m_{\text{rect}-j}}} = \frac{\sum_{x=L,y=B}^{x=R,y=T} I_{x,y}}{n(I_{x,y} > 0)} \text{ where } I_{x,y} > 0 \quad (2)$$

3. Repeat this for every time point t

We note that this method can only reliably capture cells that remain largely stationary throughout the entire acquisition sequence since the cell contours are defined once and then not updated anymore. This method generates an array of F_v/F_m single-cell values between $\{0,1\}$ with n_{cells} rows and $n_{\text{iterations}}$ columns. These values are saved into a text file, with every row representing a cell with its given index and every column representing a single time point. The output file also contains a header portion showing the used PAMalysis settings. Output also includes all raw F_v/F_m image stacks in .tif format, an image of the calculated cell mask and an indexed cell mask that relates the index in the text-results to the image data. Optionally, PAMalysis can also create the following graphs (examples shown in Figure 5): (i) Per-cell F_v/F_m over time, (ii) mean F_v/F_m of all cells over time, or (iii) a histogram of F_v/F_m for all cells at a given time. Lastly, PAMalysis creates a collated text file containing the F_v/F_m from all cells across all positions. Unless stated otherwise, all data presented was analyzed using PAMalysis.

2.8 | Calculation of throughput

Using only ImagingWin an operator can, by use of the timer functionality and by manually moving the stage position, image multiple positions, exporting them individually and then concatenating these after

the experiment is finished. With this method it is in theory possible to generate multi-dimensional data but it requires constant manual operation by the user. It also creates $n \times t$ files where n is the number of positions imaged and t is the number of times each position is imaged, all of which need to be manually concatenated.

To show how PACMan expedites this process, we take as an example the experiment in Figure 5 where six positions were imaged at 5 min intervals with a 15 s rest between positions for ~12 h. To conduct a similar experiment manually, an operator would need to manually adjust the stage position every 15 s and return to the same position every 5 min for 12 h, a nearly impossible task. To set up the correct parameters in ImagingWin/PACMan for this experiment took ~30 min and another ~30 min were spent selecting the optimal XY positions. With PACMan an operator thus spends 1 h to conduct an experiment running for 12 h.

To analyze the resulting images requires the user to select individual ROIs in ImagingWin, which approximately takes 10–20 s for a skilled operator. Selecting, verifying and exporting 100 ROI (which is the ROI limit in ImagingWin) thus takes approximately 30 minutes. In our microfluidic devices, a single image contains up to 1000 cell traps per field of view. The analysis of every cell trap (assuming an average loading rate of single cells of ~40% [9]) would imply that 400 individual ROIs needs to be selected. An operator would thus spend 1.5–2 h per image manually selecting ROIs and exporting data.

In contrast, selecting ROIs via PAMalysis and performing single-cell analysis is much faster. Here, analyzing a single image file takes 3.43 ± 0.05 ($n = 100$) seconds and analyzing all six fields of views (Figure 5) simultaneously (by using PAMalysis's batch mode) takes 22.0 ± 0.18 ($n = 100$) seconds. Analysis of the same dataset manually would require 9 h or ~ 32,000 s. The increase in throughput by using PAMalysis is thus $\frac{22 \text{ seconds}}{32\,000 \text{ seconds}} = 1454 \times$.

2.9 | Statistical analysis

Image and statistical analysis was performed with the Scikit-image [15], SciPy [16], Numpy [17] and OpenCV [18] packages in Python 3.8. Graphs were produced using the 2D-graphical plotting package Matplotlib [19] for Python.

2.10 | Software availability

PACMan and PAMalysis has been made available as an open-source software on Github and deposited as a python package via the Python Package Index (PyPi) at <https://pypi.org/project/IPAM-PACMan/>

PAMalysis can be downloaded via our Github repository at <https://github.com/OllePonten/PAMalysis/>

3 | RESULTS

Here we present a unique software suite, consisting of PACMan and PAMalysis, for the automated acquisition and analysis of microscopy-

PAM images. PACMan controls the movement and image acquisition of a commercial MICROSCOPY-PAM system (Figure 1 and Figure 2). In our experiments, PACMan increased experimental throughput 10-fold, from previously 50–300 cells per experiment to 2000–3000 cells. This microscopy automation tool is augmented with PAMalysis, a Python-based script that provides fast, unbiased, automated analysis of single-cell F_v/F_m , while increasing analysis throughput by >1400x. (Figure 3). In the following section, we first compare the accuracy of our developed analysis pipeline to that of the original software, and secondly, report experimental results that highlight the ability of our software suite to achieve the high-throughput photophysiological characterization of individual microalgae cells over time and across multiple positions.

To illustrate how PACMan expedites single-cell PAM experiments, we first recapitulate how the new method compares to the previous (manual) method. With the manual method, an operator would find a position and record cell activities at this position via the timer function in ImagingWin. This would result in a single position imaged t times, where $t = \text{length of the experiment} / \text{wait period between images}$. This method samples the temporal domain but does not allow for spatial movements between positions (Figure 3A, left). Alternatively, the operator could choose to visit and image n positions manually, typically only once (Figure 3A, right), sampling the spatial domain but not the temporal domain.

By use of PACMan, the operator can instead record multiple positions, set a wait period between positions and acquisition rounds and start the experiment and leave the instrument. PACMan will generate time-series imaging data for every position and capture data about n positions at t times (Figure 3B). This permits the operator to achieve a higher spatio-temporal resolution when compared to manual acquisition using ImagingWin.

3.1 | Benchmarking the performance of PAMalysis vs. ImagingWin

To gauge the accuracy of PAMalysis we validated whether F_v/F_m values generated by PAMalysis were comparable with those created by ImagingWin, the manufacturer-supplied software. To this end, individual cells ($n = 100$) were selected by PAMalysis and the resulting ROIs used to manually select the same cells within the ImagingWin software. Comparing both datasets revealed that the median- and maximal difference of F_v/F_m values between both software platforms was 0.45% and 1.21%, respectively, while the 95th percentile difference was 0.91%. PAMalysis is shown to slightly underestimate F_v/F_m (Figure 4).

3.2 | PACMan can monitor the photophysiology of >1000 individual microalgae across multiple positions

To experimentally test the ability of PACMan to continuously return to the same position and measure single-cell F_v/F_m , we immobilized individual microalgae (*Effrenium voratum*) within microfluidic devices

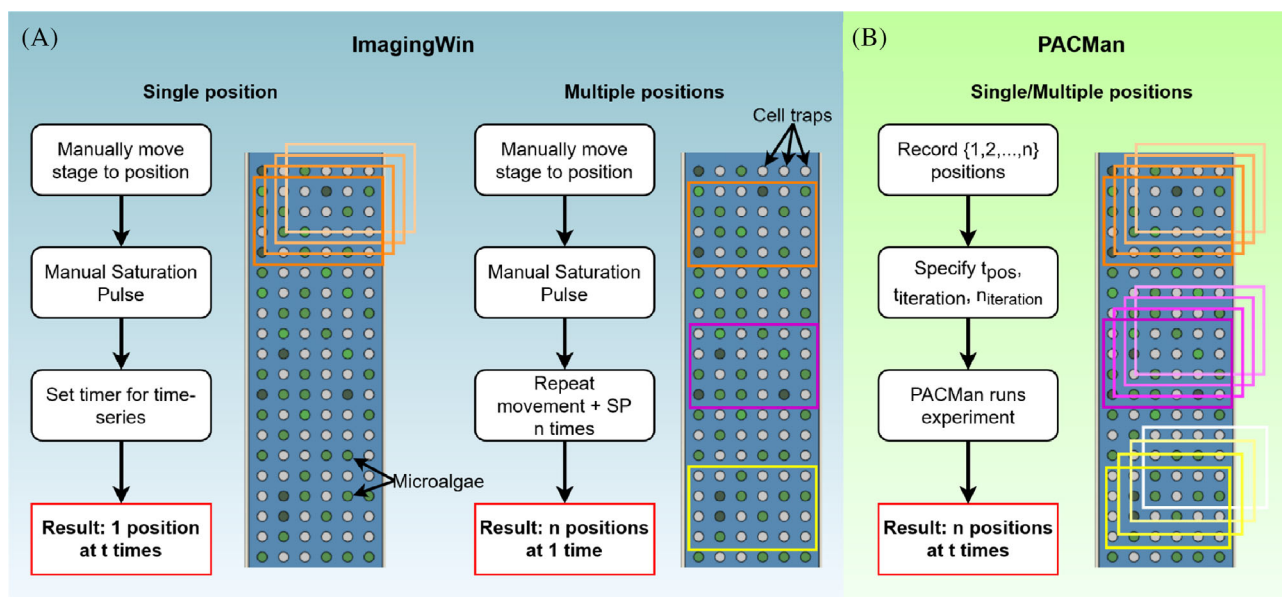


FIGURE 3 Comparison between ImagingWin and PACMan, two software packages interfacing with the MICROSCOPY-PAM system. (A) Left: For a single position experiment, the standard ImagingWin method (supplied by the manufacturer) requires the operator to manually navigate to a single position and then trigger a saturation pulse. The pulse can be triggered manually or, optionally, by using the built-in timer function that allows for repeated imaging of the same position. Right: To image multiple positions the operator needs to manually move to every position and trigger a saturation pulse and save it into a new .pim data file every time, sampling n positions at a single time point. (B) By using PACMan the operator sets PAM settings, picks a project name, determining the amount of acquisition rounds ($n_{\text{iteration}}$) and waiting periods between positions (t_{position}) and acquisition rounds ($t_{\text{iteration}}$). Positions also need to be selected according to the procedure in Figure 1. After this initial setup, the experiment can be started and PACMan will image the positions, sampling n positions at t time points. After the experiment is finished the data can be analyzed with the PAMalysis software. [Color figure can be viewed at wileyonlinelibrary.com]

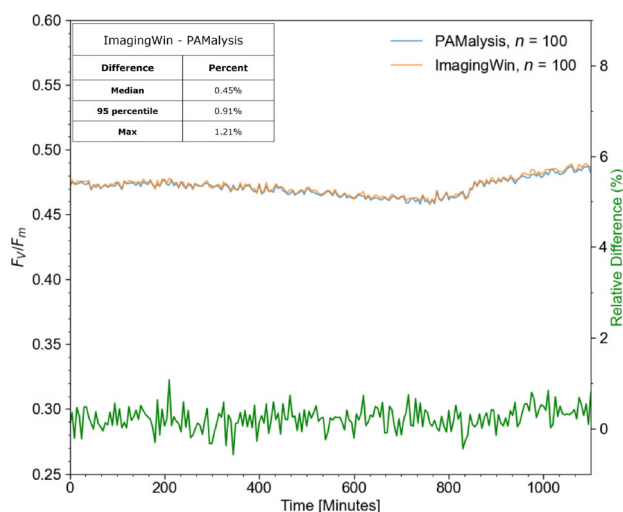


FIGURE 4 Comparison of data analyzed via PAMalysis versus imaging Win. The blue trendline is the average of the F_v/F_m of all cells automatically picked by PAMalysis. Cells selected automatically by the PAMalysis software were manually selected in ImagingWin (V 2.51D), and the red trendline is the average F_v/F_m of these manually selected cells analyzed using the ImagingWin software. The green line is the relative difference between F_v/F_m values originating from the two analysis systems: Relative Difference: $\frac{F_v/F_m(\text{ImagingWin}) - F_v/F_m(\text{PAMalysis})}{(F_v/F_m(\text{ImagingWin}) + F_v/F_m(\text{PAMalysis}))/2}$. The median difference is 0.45%, with a 95-percentile difference of 0.91%. [Color figure can be viewed at wileyonlinelibrary.com]

and imaged them over a time span of 10 h. In this experiment, (Figure 5) cells at six different positions were imaged over 121 separate acquisition rounds, resulting in a total of 3630 applied saturation pulses and corresponding F_0/F_m image pairs recorded over an area of approximately 3×3 cm. In this way, the F_v/F_m values of 2430 cells were monitored and tracked (Figure 5). This revealed that the mean F_v/F_m of all positions at $t = 0$ min was 0.419 ± 0.0569 (standard deviation, S.D.) and decreased by $\sim 16.7\%$ after 600 min, to 0.351 ± 0.0578 (S.D.).

Next, we investigated whether PACMan can be used to rapidly screen for the effect of varying chemical concentrations at the single-cell level. To this end, we loaded individual cells of the green-algae *Chlamydomonas reinhardtii* into the microwells of a microfluidic device and exposed cells to a gradient of the herbicide DCMU (see Materials and Methods, Figure S1). Using PACMan, we imaged eight positions in a 4×2 grid with a $100 \mu\text{m}$ overlap, yielding a total area of 13.2 cm^2 ($3000 \times 4400 \mu\text{m}$). Across the entire area a total of 446 individual cells were imaged. A cells position was used to determine the specific DCMU concentration it was exposed to (see Materials and Methods) and allowed us to investigate the effect of different concentrations on single-cell F_v/F_m . The global position of cells in different fields of view were extracted by analysis with PAMalysis with the global_coordinates setting set to "on".

This experiment demonstrated that increasing concentrations of DCMU decreased average F_v/F_m among cells of *C. reinhardtii*.

FIGURE 5 Experimental results from overnight imaging of individual *E. voratum* cells immobilized in a microfluidic device. All graphs were created via PAMalysis. The total duration of the experiment was 600 min and images were acquired every 5 min. (A) Images from position number three at $t = 0$ min. Clockwise from upper-left: F_0 image, F_m image, calculated F_v/F_m image, segmented and indexed cell mask. (B) F_v/F_m traces for cells shown in panel A/B/C. (C) Population averages of F_v/F_m from six independent positions over 600 min. (D) Comparison of the distribution of F_v/F_m at the start of the experiments vs. after 45 min. [Color figure can be viewed at [wileyonlinelibrary.com](https://onlinelibrary.wiley.com)]

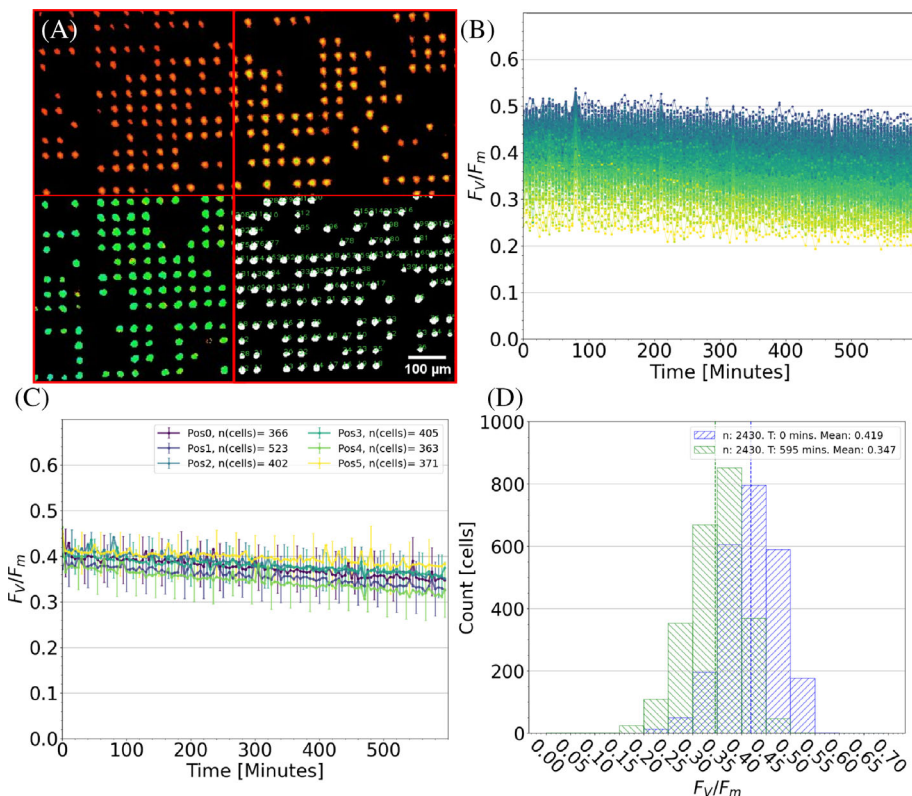
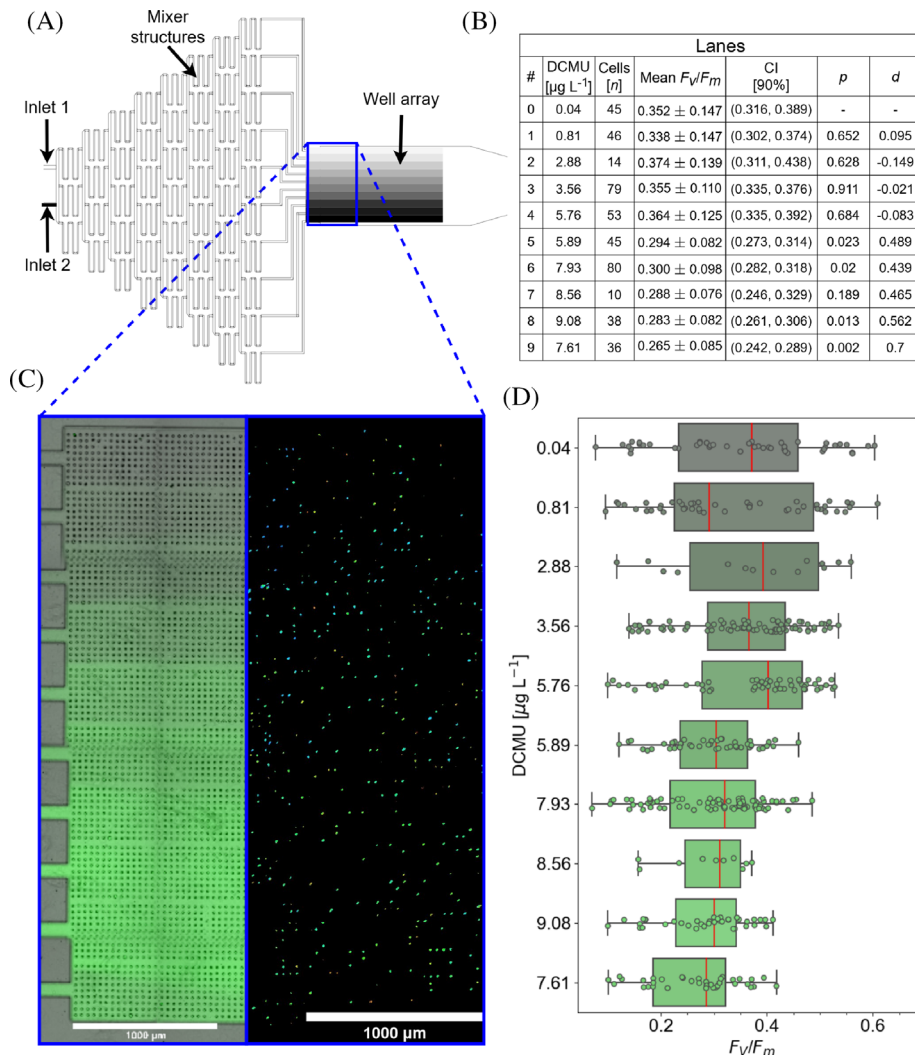


FIGURE 6 A gradient of the photosynthesis inhibitor DCMU and its effect on the photophysiology of *C. reinhardtii*. (A) Schematic of the Christmas tree gradient generator and part of the microwell array used to immobilize individual cells of microalgae. Every lane contains 1600 cell traps and covers a $7000 \mu\text{m}$ by $375 \mu\text{m}$ area. (B) Table showing statistics for the 10 “Lanes” imaged in the experiment. Mean F_v/F_m refers to average \pm standard deviation. n refers to number of cells within a specific lane. Cohen's d and p -values are calculated between every lane and the control lane (Lane 0). (C) Brightfield and fluorescence image showing part of microwell array. Fluorescence images were created using a FITC specific filter set and an excitation wavelength of 480 nm. Large image scan of eight F_v/F_m images acquired via PACMan. Total cells imaged: 446. (D) Distribution of single-cell F_v/F_m values under increasing DCMU concentrations. Median shown as red line. [Color figure can be viewed at [wileyonlinelibrary.com](https://onlinelibrary.wiley.com)]



Specifically, a DCMU concentration of $0.04 \mu\text{g L}^{-1}$ (= control, Lane 0, Figure 6C) resulted in average F_v/F_m values of 0.352 ± 0.147 ($n = 45$) whereas a DCMU concentration of $9.08 \mu\text{g L}^{-1}$ (Lane 9, Figure 6C) resulted in average F_v/F_m values of 0.289 ± 0.085 ($n = 36$) (Figure 6C). Due to non-ideal mixing the final lane experienced lower chemical concentration than expected ($7.61 \mu\text{g L}^{-1}$ as opposed to $\sim 10 \mu\text{g L}^{-1}$), but as the gradient was stable and concentration values could be calculated throughout the experiment, the data was deemed to be suitable for analysis. One-way ANOVA testing revealed a statistically significant ($p < 0.05$) decrease in F_v/F_m from 0.352 to 0.294 ($5.89 \mu\text{g L}^{-1}$), 0.300 ($7.93 \mu\text{g L}^{-1}$), 0.288 ($8.56 \mu\text{g L}^{-1}$), 0.283 ($9.08 \mu\text{g L}^{-1}$) and 0.265 ($7.61 \mu\text{g L}^{-1}$), respectively. Calculation of Cohen's d for effect size revealed the effect size varied widely between lanes but with a generally increasing trend with the concentration of DCMU [20]. The calculated effect size values are listed in Figure 6B.

4 | DISCUSSION

In a recent study, a combination of microfluidics and chlorophyll fluorescence microscopy provided insight into the life cycle of microalgae and correlated changes in photophysiology [21]. While the microfluidic device in this study contained a large number of cell traps the researchers could only image a small subset due to the technical limitations of their MICROSCOPY-PAM system. Similarly, using MICROSCOPY-PAM, we recently demonstrated that single cells of microalgae exhibit a large degree of photophysiological heterogeneity in response to thermal stress and that this heterogeneity increases under increasing temperatures [22]. These studies highlight the power of studying single cells, but also the time-consuming nature of these experiments (the data presented in our earlier study took ~ 4 months to generate, and could in theory be generated in 2 weeks using PAC-Man). Furthermore, using PAMalysis, data can be analyzed rapidly while reducing operator bias caused by the manual selection of ROIs. The capability of PAMalysis to automatically include metadata (such as the XY coordinates of positions) provides extra software functionality, as exemplified in the setup where individual *C. reinhardtii* cells were exposed to different concentrations of DCMU.

5 | CONCLUSION

There is an increasing need to understand the phenotypic heterogeneity among individual cells. Phenotypic variance among individuals, for example, allows populations to better tolerate environmental stress [23, 24] which can affect survival outcomes upon external perturbations. Yet, assessing the phenotypes of individual cells is technically challenging and requires optical interrogation methods that, ideally, provide quantitative insights into single-cell metabolism. In this context, MICROSCOPY-PAM is an ideal method as it can provide direct insights into, for example, the long-term effect of stress on the photophysiological plasticity of individuals. PACMan enables the

assessment of single-cell photophysiology at a significantly higher throughput, by integrating the control of this instrument with a motorized stage. We anticipate that this improved throughput will prove valuable to researchers seeking to advance single-cell microalgae research. This increased experimental capacity could thus facilitate investigations into phenotypic heterogeneity among natural- and commercially used microalgae, thereby aiding in the assisted evolution of coral-associated dinoflagellates [25] and microalgae used in industry [26, 27].

AUTHOR CONTRIBUTIONS

Olle Pontén: Conceptualization; writing – review and editing; performed experiments; software; investigation; validation; visualization; writing – original draft; methodology; formal analysis. **Linhong Xiao:** Methodology; data curation; investigation; resources; writing – review and editing. **Jeanne Kutter:** Methodology; validation; software; writing – review and editing. **Yuan Cui:** Methodology; resources. **Carolina Wählby:** Conceptualization; software; formal analysis; supervision; writing – review and editing. **Lars Behrendt:** Project administration; writing – review and editing; software; supervision; investigation; visualization; writing – original draft; funding acquisition; methodology; formal analysis.

ACKNOWLEDGMENTS

3D printing was performed at U-PRINT: Uppsala University's 3D-printing facility at the Disciplinary Domain of Medicine and Pharmacy and SciLifeLab Uppsala. LB was supported by grants from the Swedish Research Council (2019-04401), the Science for Life Laboratory and the Carl Trygger Foundation (CTS 20:214). We thank the Swedish Phytogeographic Society for their grant from the Lundmans Foundation (2021).

CONFLICT OF INTEREST STATEMENT

None of the authors have any conflicts of interest to declare.

DATA AVAILABILITY STATEMENT

PACMan is available as a Python package at <https://pypi.org/project/IPAM-PACMan/>. PAMalysis is available at <https://github.com/OllePonten/PAMalysis>.

ORCID

Olle Pontén  <https://orcid.org/0000-0002-8061-2060>

Carolina Wählby  <https://orcid.org/0000-0002-4139-7003>

Lars Behrendt  <https://orcid.org/0000-0002-8988-2032>

REFERENCES

1. Baker NR. Chlorophyll fluorescence: a probe of photosynthesis in vivo. *Annu Rev Plant Biol.* 2008;59:89–113.
2. Suresh Kumar K, Dahms HU, Lee JS, Kim HC, Lee WC, Shin KH. Algal photosynthetic responses to toxic metals and herbicides assessed by chlorophyll a fluorescence. *Ecotoxicol Environ Saf.* 2014;104:51–71.
3. Steinberger I, Egidi F, Schneider A. Chlorophyll fluorescence measurements in Arabidopsis wild-type and photosystem II mutant leaves. *Bio-Protoc.* 2015;5:e1532.

4. Song X, Zhou G, Xu Z, Lv X, Wang Y. Detection of photosynthetic performance of *Stipa bungeana* seedlings under climatic change using chlorophyll fluorescence imaging. *Front Plant Sci.* 2016;6:1254. Available at. <https://www.frontiersin.org/articles/10.3389/fpls.2015.01254>
5. Liberman R, Fine M, Benayahu Y. Simulated climate change scenarios impact the reproduction and early life stages of a soft coral. *Mar Environ Res.* 2021;163:105215.
6. Linn AI, Zeller AK, Pfündel EE, Gerhards R. Features and applications of a field imaging chlorophyll fluorometer to measure stress in agricultural plants. *Precis Agric.* 2021;22:947–63.
7. Genty B, Briantais JM, Baker NR. The relationship between the quantum yield of photosynthetic electron transport and quenching of chlorophyll fluorescence. *Biochim Biophys Acta BBA - Gen Subj.* 1989; 990:87–92.
8. Dani KGS, Pollastri S, Pinosio S, Reichelt M, Sharkey TD, Schnitzler J-P, et al. Isoprene enhances leaf cytokinin metabolism and induces early senescence. *New Phytol.* 2022;234:961–74.
9. Behrendt L, Salek MM, Trampe EL, Fernandez VI, Lee KS, Kühl M, et al. PhenoChip: a single-cell phenomic platform for high-throughput photophysiological analyses of microalgae. *Sci Adv.* 2020;6: eabb2754. <https://doi.org/10.1126/sciadv.abb2754>
10. Herdean A, Sutherland DL, Ralph PJ. Phenoplate: an innovative method for assessing interacting effects of temperature and light on non-photochemical quenching in microalgae under chemical stress. *N Biotechnol.* 2022;66:89–96.
11. Edelstein A, Amodaj N, Hoover K, Vale R, Stuurman N. Computer control of microscopes using μ Manager. *Curr Protoc Mol Biol*, 2010. Chapter 14:Unit14.20. <https://doi.org/10.1002/0471142727.mb1420s92>
12. Trampe E, Kolbowski J, Schreiber U, Kühl M. Rapid assessment of different oxygenic phototrophs and single-cell photosynthesis with multicolour variable chlorophyll fluorescence imaging. *Mar Biol.* 2011; 158:1667–75.
13. Heinz Walz GmbH, IMAGING-PAM M-Series Chlorophyll Fluorometer - Instrument Description and Information for Users. Effeltrich, Germany (2019).
14. Suzuki S, Abe K. Topological structural analysis of digitized binary images by border following. *Comput Vis Graph Image Process.* 1985; 30:32–46.
15. van der Walt S, Schönberger JL, Nunez-Iglesias J, Boulogne F, Warner JD, Yager N, et al. Scikit-image: image processing in python. *PeerJ.* 2014;2:e453.
16. Virtanen P, Gommers R, Oliphant TE, Haberland M, Reddy T, Cournapeau D, et al. SciPy 1.0: fundamental algorithms for scientific computing in Python. *Nat Methods.* 2020;17:261–72.
17. Harris CR, Millman KJ, van der Walt SJ, Gommers R, Virtanen P, Cournapeau D, et al. Array programming with NumPy. *Nature.* 2020; 585:357–62.
18. Bradski G. The OpenCV library. Tools: Dr Dobbs J. Softw; 2000.
19. Hunter JD. Matplotlib: a 2D graphics environment. *Comput Sci Eng.* 2007;9:90–5.
20. Baguley T. Standardized or simple effect size: what should be reported? *Br J Psychol.* 2009;100:603–17.
21. Széles E, Nagy K, Ábrahám Á, Kovács S, Podmaniczki A, Nagy V, et al. Microfluidic platforms designed for morphological and photosynthetic investigations of *Chlamydomonas reinhardtii* on a single-cell level. *Cell.* 2022;11:285.
22. Xiao L, Johansson S, Rughöft S, Burki F, Sandin MM, Tenje M, et al. Photophysiological response of Symbiodiniaceae single cells to temperature stress. *ISME J.* 2022;16:2060–4.
23. Hughes AR, Stachowicz JJ. Genetic diversity enhances the resistance of a seagrass ecosystem to disturbance. *Proc Natl Acad Sci U S A.* 2004;101:8998–9002.
24. Sjöqvist CO, Kremp A. Genetic diversity affects ecological performance and stress response of marine diatom populations. *ISME J.* 2016;10:2755–66.
25. Buerger P, Alvarez-Roa C, Coppin CW, Pearce SL, Chakravarti LJ, Oakeshott JG, et al. Heat-evolved microalgal symbionts increase coral bleaching tolerance. *Sci Adv.* 2020;6:eaba2498.
26. Zhang B, Wu J, Meng F. Adaptive laboratory evolution of microalgae: a review of the regulation of growth, stress resistance, metabolic processes, and biodegradation of pollutants. *Front Microbiol.* 2021) Available at;12:737248. <https://www.frontiersin.org/articles/10.3389/fmicb.2021.737248>
27. Pontén O. PACMan: an automated chlorophyll-a fluorescence acquisition platform for single cell microalgae analysis. Uppsala: Uppsala University; 2021.

SUPPORTING INFORMATION

Additional supporting information can be found online in the Supporting Information section at the end of this article.

How to cite this article: Pontén O, Xiao L, Kutter J, Cui Y, Wählby C, Behrendt L. PACMan: A software package for automated single-cell chlorophyll fluorometry. *Cytometry.* 2024;105(3):203–13. <https://doi.org/10.1002/cyto.a.24808>